The effects of intestinal air cavity on dose distribution of volume modulated arc therapy for cervical cancer

Xiaobin Chang[1]^, Yuan Yuan[2], Guoqing Wang[2], Lijuan Hu[2], Min Zhou[2], Huijuan Liu[1], Libo Pan[3], Jing Wang[2]

[1]Department of Radiation Oncology, Shaanxi Provincial Tumor Hospital, Affiliated Hospital of Xi'an Jiaotong University Health Science Center, Xi'an, China; [2]Department of Gynaecological Oncology, Shaanxi Provincial Tumor Hospital, Affiliated Hospital of Xi'an Jiaotong University Health Science Center, Xi'an, China; [3]Department of Computed Tomography, Shaanxi Provincial Tumor Hospital, Affiliated Hospital of Xi'an Jiaotong University Health Science Center, Xi'an, China

Contributions: (I) Conception and design: X Chang; (II) Administrative support: L Hu; (III) Provision of study materials or patients: G Wang; (IV) Collection and assembly of data: Y Yuan; (V) Data analysis and interpretation: X Chang; (VI) Manuscript writing: All authors; (VII) Final approval of manuscript: All authors.

Correspondence to: Lijuan Hu. Department of Gynaecological Oncology, Shaanxi Provincial Tumor Hospital, Affiliated Hospital of Xi'an Jiaotong University Health Science Center, Xi'an 710061, China. Email: 251337993@qq.com.

Background: This study explored the effects of air cavity on the dose distribution of radiotherapy in patients after extensive hysterectomy. In patients who have an air cavity in the intestines near the planning target volume (PTV), the photon beams may interact with the air cavity to cause electron disequilibrium (ED), resulting in a reduction in the absorbed dose by the surrounding tissues. In this paper, the electron density assignment (EDA) of the air cavity was used to simulate the disappearance of the intestinal gas, and the effects of the intestinal air cavity on the volume modulated arc therapy (VMAT) results were examined.

Methods: A total of 21 patients who underwent VMAT after extensive hysterectomy were enrolled in this retrospective analysis. The dose parameters from the selected treatment plan were used the experimental reference. The treatment plan of the reference group was copied, and the intestinal air cavity structure was identified using the computed tomography (CT) simulation image. The electron density value of the intestine near the cavity was measured and averaged according to the intestinal electron density value recommended by International Commission Radiological Units (ICRU) report No. 46. The averaged value was assigned to the air cavity structure. Subsequently, the treatment plan was re-calculated without changing other parameters, and the resulting treatment plan was defined as the experimental group. The dose parameters of the PTV and organs at risk (OAR) in the 2 groups were assessed, and the influence of the intestinal air cavity on the VMAT dose distribution in cervical cancer patients was analyzed.

Results: The minimum dose (D_{98}) and the maximum dose (D_2) of the PTV was significantly different between the experimental group and the control group (P<0.05), however, mean dose of the PTV was comparable between the 2 groups. The dose parameters of OARs were not significantly different between the two groups except the bone structural organs.

Conclusions: When the intestinal air cavity is large and related to the target area, the intestinal air cavity should be intervened, and the patient should be treated with radiotherapy after the intestinal gas decreases.

Keywords: Volume modulated arc therapy (VMAT); air cavity; cervical cancer; dose distribution

^ ORCID: 0000-0003-0038-0464.

Introduction

In some cervical cancer patients who undergo extensive hysterectomy followed by radiotherapy, there is a severe build up of intestinal gas, visible via computed tomography (CT) simulation images. The most common causes of this gastrointestinal gas include functional dyspepsia, irritable bowel syndrome, and chronic idiopathic constipation (1). Patients with lactose intolerance also experience serious intestinal gas build up due to the excessive growth of small intestinal bacteria (2). During abdominal surgery, factors such as intestinal traction, exposure, anesthesia, and trauma, can lead to gastrointestinal dysfunction, manifesting as weakened or absent bowel movements, abdominal distension, or flatulence. Under normal circumstances, gastrointestinal function will recover after 24 to 72 hours postoperatively. However, some patients will still experience abdominal distension due to intestinal function, diet, and bacterial imbalance (3,4). Intestinal flatulence not only causes discomfort to the patient, but can also adversely affects the patient's subsequent radiotherapy.

The usual treatment regimen for patients with cervical cancer is extensive hysterectomy followed by external radiation therapy three weeks later to consolidate the surgical effect. During radiotherapy, the radiotherapist determines the range of the target area based on CT simulation images and outlines the organs that need to be protected. The electron density measurements corresponding to different CT values obtained from the CT simulation image is used to calculate the dose distribution in the patient's body. When there are air cavities present in the intestines near the treatment target area, the photon beams used in external radiotherapy will pass through these cavities causing electron disequilibrium (ED). When the number of charged particles entering a volume of medium is equal to the number of particles leaving the same volume, it is called the electron equilibrium state, otherwise the ED phenomenon will occur (5). Ostwald *et al.* applied the 6 megavolt (MV) photon beam opposed lateral fields radiation technique to study the influence of air cavities on the radiation dose in the larynx. The results of thermoluminescence dose measurement showed that the ED phenomenon can cause an average 6–18% drop in the dose reaching the mucosal tissue in the larynx (6,7). Huang *et al.* set up air cavities of different sizes in the acrylic plastic phantom and demonstrated via the Monte Carlo simulation that the convolution/superposition dose calculation algorithm can overestimate the dose inside the phantom

air cavity, especially for the built-up area of the phantom cavity. The greatest impact depth was observed with a depth of up to 0.5 cm (8). Other studies have also examined the influence of the ED phenomenon on the radiotherapy dose delivered. The lungs (9,10), upper respiratory tract mucosal tissues (11), and air cavities can all have an impact on the patient's radiation therapy dose distribution. Thus, the effects of air cavities, observed via CT simulation images, during volume modulated arc therapy (VMAT) radiotherapy of cervical cancer patients should be investigated.

To study the dosimetric difference between the presence and absence of intestinal air cavities in cervical patients undergoing radiotherapy after extensive hysterectomy, this investigation used the electron density assignment (EDA) method to simulate the disappearance of the intestinal air cavity. The EDA method is often used in the research of radiation therapy dosimetry. In recent years, magnetic resonance imaging (MRI) guided radiotherapy technology has gained much attention. One of the main limitations of using MRI alone in treatment planning is the lack of correlation between the MRI signal intensity and electron density. However, the electron density of different human tissues is a necessary parameter for dose calculation. One of the simplest but very effective solutions is to assign electron density values to the treatment target area, organs at risk (OAR), and the normal tissues in the MRI image, so that the relative relationship between the MRI signal intensity and the electron density value can be established (12-15). Oral contrast agents are commonly used in the diagnosis of abdominal lesions, as they make the intestinal tube display high density in CT images. After the contrast agent is discharged from the body, the density of the bowel returns to normal. Some studies have also used the EDA method to examine the influence of intestinal contrast media on the radiation therapy dose (16,17). Metal artifacts observed on CT images can also affect the distribution of the radiation treatment dose. Maerz *et al.* used the EDA method to assign the normal electron density to the artifact area according to the International Commission on Radiological Protection (ICRP) report 23 and the International Commission on Radiological Units (ICRU) report 44 on the recommended value of the standard organization's electron density relative to water. The authors then compared the accuracy of the dose calculation using the treatment plan system (18). Our current study also used the EDA method to assign the normal intestinal electron density value to the air cavity observed on the radiotherapy CT simulation image. The value of the electron density of the bowel was determined
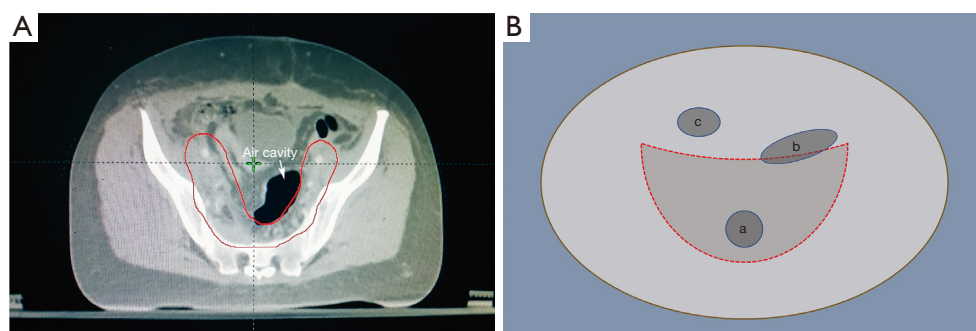
Figure 1 A schematic diagram showing the introduction of the air cavity in the coronal plane of the CT image and the phantom. (A) Patient coronal section; (B) Phantom coronal section. The red area denotes the range of the PTV, while a, b, and c denotes the air cavity in different positions of the phantom. Air cavity a and b meet the enrollment criteria, while air cavity c does satisfy the criteria. CT, computed tomography; PTV, planning target volume.

according to the recommended value in the ICRU 46 report (19). The dose was recalculated without changing the original parameters of the radiation treatment plan, and the influence of the absence of the air cavity on the dose distribution of the treatment plan was analyzed.

Previous studies examining the larynx cavity (6), the cavity in the phantom (8), and the upper respiratory tract cavity (11) have shown that the existence of the air cavity will affect the radiation treatment dose in the cavity and its surrounding tissues. However, most of these studies were conducted on the basis of a single field or two opposed lateral fields and a single case. This article used VMAT technology to study the effects of intestinal air cavity on the results of the radiotherapy treatment plan in cervical cancer patients after extensive hysterectomy. The advantages of using VMAT technology include more beam segments, increased beam directions, a variable dose rate, and variable gantry speed. Popescu *et al.* (20) demonstrated a more favorable dose distribution to the target and OARs, with reduced monitor units using VMAT compared with conventional fixed fields IMRT. The difference in the dose distribution achieved with the same treatment plan parameters was compared in the presence and absence of the air cavity on CT simulation images. We present the following article in accordance with the MDAR reporting checklist (available at https://apm.amegroups.com/article/view/10.21037/apm-22-66/rc).

Methods

Clinical data and target contouring

Clinical data

A total of 21 cervical cancer patients who underwent radiotherapy treatment in Shaanxi Provincial Tumor Hospital, Affiliated Hospital of Xi'an Jiaotong University Health Science Center from March 2018 to May 2021 after extensive hysterectomy and pelvic and abdominal aortic lymph node dissection were retrospectively enrolled in this study. The patients ranged from 38–66 years old, with a median age of 47 years. None of the patients had contraindications to radiotherapy and all signed informed consents for radiotherapy. All radiotherapy treatment procedures were completed without interruption during the treatment period. Patients whose CT simulation image data showed the presence of overlapping areas between the air cavity and the planning target volume (PTV) boundary line were included in this study (*Figure 1*). If the air cavity does not lie within the PTV or the cavity does not intersect with the PTV boundary line, the enrollment criteria was not satisfied and the patients were excluded. Due to the retrospective nature of this study, only the dosimetry data of the treatment plan was collated, and there was no intervention with the patient's actual treatment. There were no potential risks during the research process and the patient's privacy was protected at all times. This study

was approved by the Medical Ethics Committee of Shaanxi Provincial Tumor Hospital (approval No. 2020-02). The study was conducted in accordance with the Declaration of Helsinki (as revised in 2013). Informed consent was provided by all patients.

Target range and delineation of the OARs
The target area delineation is performed according to the Radiation Therapy Oncology Group (RTOG) target area delineation guide for intensity-modulated radiation therapy (IMRT) radiotherapy after cervical cancer surgery. The clinical target volume (CTV) delineation includes the tumor bed after tumor resection and the related lymphatic drainage area. The PTV area is generated by expanding the obtained CTV area 1 cm up, down, and ventral to the patient, and expanding the area 0.5 cm to the left, right, and back (21). The delineation of the OARs is performed according to the RTOG pelvic normal tissue delineation guidelines, including the small intestine, bladder, rectum, colon, femoral head, and spinal cord (22). The gas cavity structures that satisfied the inclusion criteria required a complete outline of the interpenetrating gas range layer by layer in the cross section of the CT image, and all air cavity structures that met the conditions in the CT image were named "air cavity".

Electron density assignment and experimental design

Electron density assignment to the air cavity
To simulate the patient's treatment conditions after the intestinal air cavity disappears, the EDA method was used to process the outlined air cavity structure. First, the electron density value E1 of the intestinal contents near the air cavity in the selected CT simulation image was measured, and then the recommended value of 1.03 for the intestinal electron density listed in ICRU Report No. 46 [gastrointestinal (GI) tract adult =1.03 kg/m^{-3}] was determined (19). The electron density E assigned to the air cavity of the CT simulation image was obtained using the following formula Eq. [1]:

$$E = \frac{E_1 + 1.03}{2} \qquad [1]$$

In the treatment plan system (Eclipse 15.6, Varian, USA), the E value was assigned using the formula Eq. [1] in the "air cavity" attribute box.
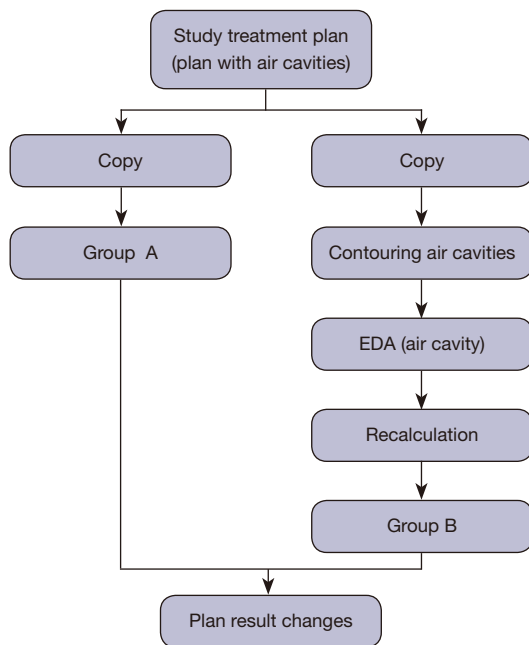
Experimental design
The treatment plans selected in this retrospective study were all designed with VMAT. The total prescription dose was 50 Gy (2 Gy per day). The photon energy was 6 MV, with a double arc design, a clockwise arc range of 181–179°, a counterclockwise arc range of 179–181°, PO (Photon Optimizer, Version 15.1.61) as the optimization algorithm, and Acuros XB as the dose calculation algorithm (Acuros External Beam, Version 15.6.06). For the target dose, 95–110% coverage of the PTV volume was required by the prescription dose. All treatment plans were delivered via the Varian Electron Linear Accelerator TrueBeam (Trubeam1697, Varian Medical Systems, Palo Alto, CA, USA). For the accuracy of the measurement results, quality control work is carried out before the measurement to confirm that the parameters of the electron linear accelerator and dosimetry equipment are within the allowable range. This experiment was divided into 4 steps. First, the dose distribution results of the selected treatment plan were recorded and used as the experimental reference. This was defined as the control group. Second, the CT simulation images were copied, along with the PTV and OAR of the treatment plan of the control group. The air cavity in the image that satisfied the experimental requirements were outlined and the results of formula Eq. [1] were applied. Values were assigned to the air cavity and this group was defined as the experimental group. Third, the control group's treatment plan was transferred without any modification to the experimental group's CT simulation image target area structure. The same dose calculation algorithm was used to recalculate the dose distribution, a new treatment plan dose distribution was generated, and the relevant parameters were recorded. Finally, statistical analyses were performed on the dose distribution of the treatment plan in the experimental group and the control group. The specific experimental flow chart is shown in *Figure 2*.

Dosimetric analysis of the air cavity in water equivalent phantom
To clearly understand the perturbation law of the air cavity to the radiation dose distribution, a water equivalent phantom experiment was designed. A water equivalent phantom of 300 mm × 300 mm was created in the Eclipse treatment planning system, in which a rectangular parallelepiped (air gap) with a thickness of 10 mm was defined, and the upper surface of the air gap was 50 mm from the surface of the water phantom (*Figure 3*). A Varian Truebeam electron linear accelerator 6 MV photon beam was used to irradiate the phantom. The dose algorithm
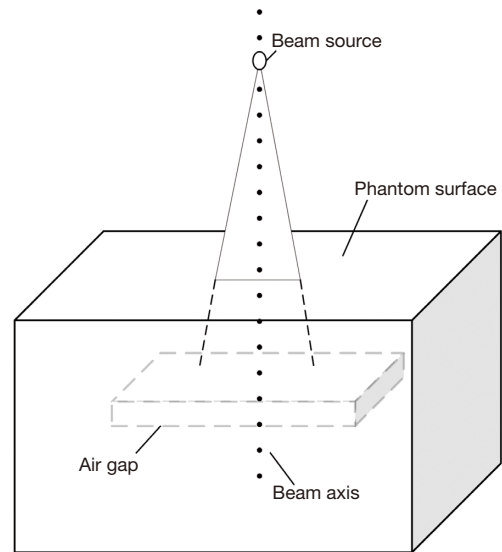
1330

Chang et al. Effects of air cavity on dose distribution

Figure 2 A flow chart showing the experimental procedure. EDA, electron density assignment.

Figure 3 A schematic diagram showing the air cavity in the water equivalent phantom.

was Acuros XB, the field size was 10 cm × 10 cm, and the distance between the photon beam source and the water equivalent phantom surface was 100 cm. The percentage depth dose of the central axis of the beam was collected to analyze the influence of the air cavity on the dose distribution of the water phantom.

Statistical analysis

According to the special characteristics of the intestinal air cavity in the selected treatment plan, the dosimetry parameters of the routine OARs in the abdomen were selected for statistical analysis, including the PTV minimum dose (D_{98}), the average dose (D_{mean}), the maximum dose (D_2), and the OAR statistics including bladder V_{40} (the percent volume of the normal organ receiving 40 Gy or more), rectum V_{40}, colon V_{40}, small intestine V_{30}, and femoral head V_{35}. All parameters are expressed as mean ± standard deviation. The Shapiro-Wilk method was used to test the normality of the data of the PTV and OAR, and all data met the requirements of normal distribution ($P>0.05$). GraphPad Prism 8.0 was used for paired t-test, and $P<0.05$ was considered statistically significant. A bar chart with error bars of the homogeneity index (HI) and conformity index (CI) of the two sample treatment plans

was constructed, and the influence of the intestinal air cavity on the results of the cervical cancer treatment plan was analyzed.

Results

The effects of air gap in the water equivalent phantom

The percentage depth dose curve of the central axis of the photon beams in the phantom was collected from the Eclipse treatment plan system. For a 10 cm × 10 cm field, the air cavity obviously changed the percentage depth dose distribution of the 6 MV photon beam. As shown in *Figure 4*, before the beam entered the air gap depth, the central axis percent depth curve of the beam field fit well with the central axis percent depth dose curve of the beam field when there was no air gap. In the air gap depth area, the phantom beam central axis percent depth dose was significantly reduced when there was an air gap, and a low valley area appeared. After the air gap depth, the phantom beam central axis percentage depth dose with an air gap was slightly higher than that without an air gap.

The effects of air cavity on the dose of the PTV

The average PTV volume of the selected treatment plans was 994.85±187.43 cm³ and the average volume of the air cavity was 121.48±58.31 cm³. According to the results of
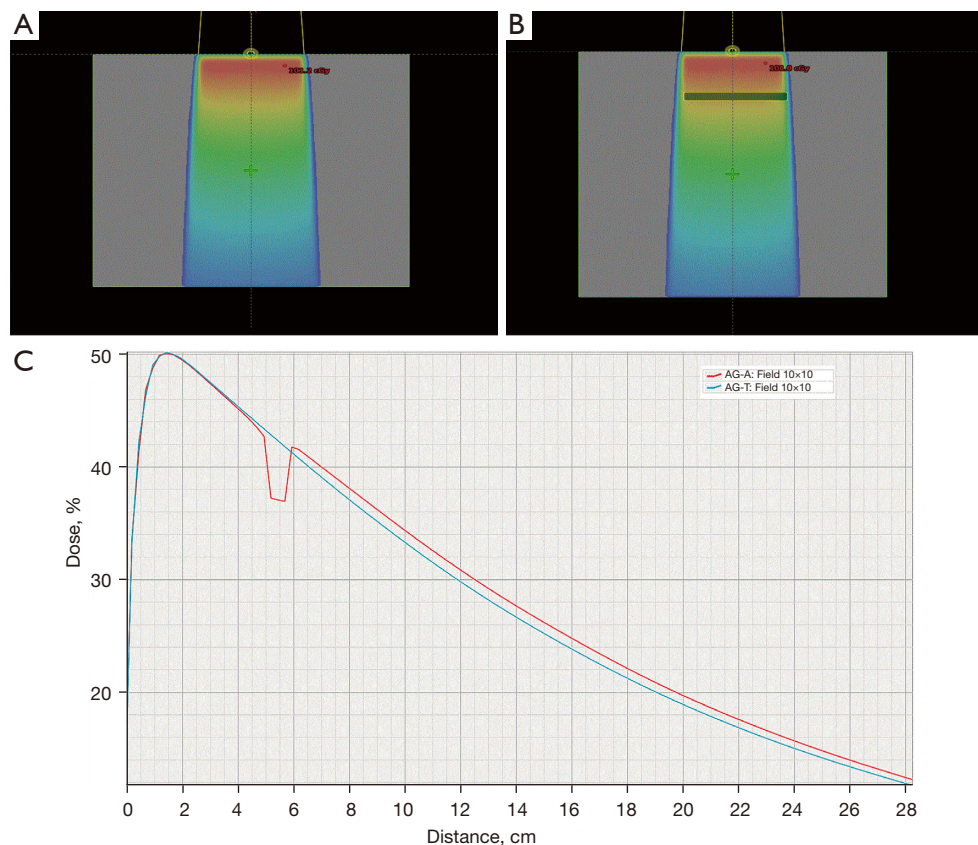
Figure 4 A schematic diagram of the water-equivalent phantom experiment and data analysis diagram. For a 10 cm × 10 cm field, the air cavity obviously changed the percentage depth dose distribution of the 6 MV photon beam. (A) The dose distribution of the photon beam in a uniform water phantom. (B) The dose distribution of the photon beam when there is an air gap in the uniform water phantom. (C) The blue line is the center axis percent depth dose curve of the water phantom photon beam, and the red line is the center axis percent depth dose curve of the water phantom when there is an air gap. MV, megavolt; AG-A, percentage depth dose containing gas cavity; AG-T, percentage depth dose without air cavity.

Table 1 The difference in the PTV dosimetric parameters between the experimental group and the control group

Parameters	Control group, mean ± SD (Gy)	Experimental group, mean ± SD (Gy)	t	P
D_{98}	49.37±0.81	49.39±0.78	−2.551	0.019
D_{mean}	52.02±0.35	52.09±0.30	−1.738	0.097
D_2	54.31±0.67	54.16±0.64	5.393	0.000

PTV, planned target volume; SD, standard deviation; D_{98}, minimum dose; D_{mean}, average dose; D_2, maximum dose.

Eq. [1], the average value of the electron density assigned to the air cavity was 1.023±0.11 g/cm^3. There was a statistically significant difference in the PTV dose parameters of D_{98} and D_2, but not D_{mean}, between the experimental group and the control group (P<0.05; *Table 1*).

The effects of air cavity on the dose of the OARs

As shown in *Table 2*, the dose volume parameters of the OARs, namely, the bladder, rectum, and small intestine, were not significantly different between the two groups.

Table 2 The difference in dosimetry parameters of the OARs between the experimental group and the control group

Parameters	Control group, mean ± SD (%)	Experimental group, mean ± SD (%)	t	P
Bladder V_{40}	42.43±14.65	42.68±14.63	−1.262	0.221
Rectum V_{40}	55.74±13.25	55.54±13.35	0.747	0.464
Intestine V_{30}	13.38±10.82	12.26±10.66	1.111	0.279
Colon V_{40}	56.84±12.94	58.11±12.06	−2.185	0.040
Femoral V_{30}	25.92±14.54	25.60±14.50	3.959	0.023

OARs, organs at risk; SD, standard deviation; V_{40}, the percent volume of the normal organ receiving 40 Gy or more; V_{30}, the percent volume of the normal organ receiving 30 Gy or more.
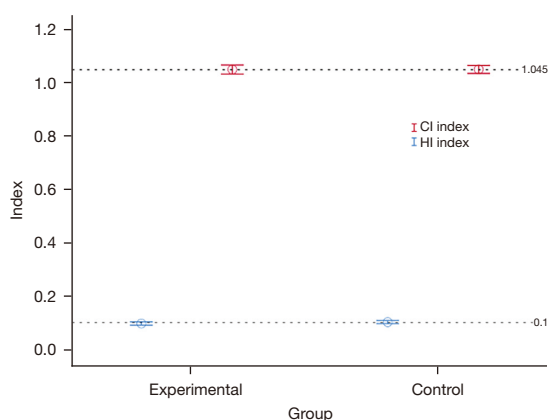
Figure 5 The error bar graphs of the CI and the HI of the experimental group and the control group. Red represents the CI index, and blue represents the HI index. CI, conformity index; HI, homogeneity index.

The difference between the colon dose volume parameter V_{40} and the femoral head dose parameter V_{30} was statistically significant (P<0.05).

The effects of air cavity on the CI and the HI

The CI and HI are commonly used indicators for evaluating the quality of treatment plans and are calculated according to the formulas listed below as proposed by Wu *et al.* (23) and Lomax *et al.* (24), respectively:

$$HI = \frac{D_2 - D_{98}}{D_{prescription}} \qquad [2]$$

and

$$CI = \frac{V_{T,ref}}{TV} \qquad [3]$$

where D_2 is the radiation dose received by 2% PTV volume (maximum dose), D_{98} is the radiation dose received by 98% PTV volume (minimum dose), and $D_{prescription}$ is the prescription dose given by the PTV. $V_{T, ref}$ is the volume of the target area greater than or equal to the reference dose (prescription dose), and TV is the volume of the PTV. In an ideal situation, the HI value approaches 0 and the CI value approaches 1.

There was no significant difference in the CI index of the treatment plan between the control group and the experimental group (P=0.222). When the treatment plan of the control group contained a cavity, the mean HI index was 0.096±0.013, and the treatment plan of the experimental group was 0.098±0.014 after the electron density of the gas cavity was assigned by the EDA method. *Figure 5* shows that the HI index of the experimental group and the control group are located below and above the index =0.1 reference line, respectively, and the difference between the two groups was statistically significant (P=0.000).

Discussion

During tumor radiotherapy, when there is an air cavity in the vicinity of the tumor, there will be a phenomenon of under-dosing in the air-tissue interface (25,26). A number of studies have demonstrated that the Acuros XB dose algorithm can better predict the dose distribution when there is an air cavity present, and the difference between this calculation result and that achieved with the Monte Carlo algorithm is within 2% (27,28). In this study, the Acuros XB dose algorithm was applied to the water-equivalent phantom experiment. The results demonstrated that, due to the existence of the air gap, the electron equilibrium state in the water equivalent phantom disappeared, and the dose inside the air cavity decreased significantly. In

addition, there were obvious secondary build-up effects on the interface between the phantom and the cavity and this agreed with previous studies (29-31). In the case of a single irradiation field, the air cavity exerted an obvious disturbing effect on the internal dose of the water phantom.

The present study showed that in terms of PTV dosimetry, there was a significant difference in both the maximum and minimum doses of PTV between the experimental group and the control group. The average dose of PTV was similar between the two groups. Except for the significant differences in the dose parameters of the colon and the femoral head between the two groups, no significant differences could be seen in the dosimetry parameters of the other OARs. Previous studies on air cavity dose distribution reported dose measurements that were performed on the beam axis, and the conclusions were drawn under the conditions of a single field or an opposed lateral field (6-10). Petoukhova *et al.* (26) quantified the air cavity effect by measuring the dose changes at the edge of the air cavity. The insufficient dose of the air cavity of a single beam or two beams can be as high as 20% and 10%, respectively. When the beam number increases, the insufficient dose gradually decreases. For VMAT, the influence of the intestinal air cavity in CT simulation images on the planned dose results of radiotherapy is more complicated, since there are many beam directions, large numbers of beam segments, and different sizes and shapes of beam segments. Taylor and Li *et al.* (32,33) used the Monte Carlo method to analyze the influence of the radiation field size on the dose distribution at the electronic imbalance air-tissue interface, and showed that the smaller the radiation field area, the greater the influence of the air cavity on the dose distribution. The author believed that, owing to various beam directions in the treatment field of VMAT technology, the lateral transport of secondary electrons inside the cavity alleviates the influence of the air cavity on the dose distribution to a certain extent. However, due to the existence of a large amount of small treatment beam segments in VMAT, when there are a large number of air cavities in the treatment area, the impact of the air cavities cannot be ignored. The HI of the treatment target area and the dose distribution of the organ where the cavity is located could be affected by the air cavity. Since the distribution of the air cavity of the selected patients in this study was mainly located in the colon, a significant difference in the dosimetry parameters between the two groups was observed in the colon. Normally, the density

of the intestine is very close within a certain range, and the change in location has less impact on the dose distribution. However, when air is present in the intestine, changes in the location of the air cavity alters the density of the intestine, which affects the dose distribution in the intestine and target areas According to our research, when the air cavity area in the CT simulation image of radiotherapy was relatively fixed and always present, such as in the rhinitis and larynx, the use of accurate dose prediction algorithm is an effective way to solve the accuracy of the delivery dose. However, when the air cavity is present in the CT simulation image for a short time, such as that caused by intestinal gas, the intestinal air cavity should be intervened to reduce or eliminated the air cavity in the CT images of the patients. This is important so as to ensure the air cavity remains in a relatively stable state. VMAT is a high-quality and efficient treatment for patients with cervical cancer. In the treatment of cervical cancer with VMAT, intervention in the patient's intestinal air cavity improves the accuracy of the patient's prescription dose.

In this investigation, the CT simulation images of patients undergoing radiotherapy after extensive hysterectomy were used to analyze the influence of air cavity on dose distribution. While this is more representative of the actual clinical conditions, there were several limitations to this study. Only the 6 MV photon rays were analyzed, and the effects of different beam energy, flattening filter free beams, electronic beams, and different dose algorithms of treatment plans were not examined. Considering the impact of retrospective analysis of cases on the results, we will actively carry out multi-center research to further study the problems of this paper. More in-depth research is warranted to determine the impact of air cavities on the outcomes of radiotherapy treatment plans.

Conclusions

When intestinal gas is present in or around the target area of cervical cancer, the influence of the gas cavity on the dose distribution of radiation therapy cannot be dismissed. The authors suggest that when there is an intestinal air cavity, the intestinal gas should be reduced or eliminated with improved diet or drug intervention if possible. When the patient's intestinal gas condition improves, radiotherapy CT simulation and radiotherapy plans can be designed. All these measures aim to reduce the uncertainty of the prescription dose of radiotherapy, increase the effect of radiotherapy,

1334

Chang et al. Effects of air cavity on dose distribution

and reduce the damage to the normal tissues.

Acknowledgments

Footnote

Reporting Checklist: The authors have completed the MDAR reporting checklist. Available at https://apm.amegroups.com/article/view/10.21037/apm-22-66/rc

Data Sharing Statement: Available at https://apm.amegroups.com/article/view/10.21037/apm-22-66/dss

Conflicts of Interest: All authors have completed the ICMJE uniform disclosure form (available at https://apm.amegroups.com/article/view/10.21037/apm-22-66/coif). The authors have no conflicts of interest to declare.

Ethical Statement: The authors are accountable for all aspects of the work in ensuring that questions related to the accuracy or integrity of any part of the work are appropriately investigated and resolved. This study was approved by the Medical Ethics Committee of Shaanxi Provincial Tumor Hospital (approval No. 2020-02). The study was conducted in accordance with the Declaration of Helsinki (as revised in 2013). Informed consent was provided by all patients.

References

1. Wilkinson JM, Cozine EW, Loftus CG. Gas, Bloating, and Belching: Approach to Evaluation and Management. Am Fam Physician 2019;99:301-9.
2. Zhao J, Fox M, Cong Y, et al. Lactose intolerance in patients with chronic functional diarrhoea: the role of small intestinal bacterial overgrowth. Aliment Pharmacol Ther 2010;31:892-900.
3. Stengel A, Taché Y. Ghrelin: new insight to mechanisms and treatment of postoperative gastric ileus. Curr Pharm Des 2011;17:1587-93.
4. Sugawara K, Kawaguchi Y, Nomura Y, et al. Perioperative Factors Predicting Prolonged Postoperative Ileus After Major Abdominal Surgery. J Gastrointest Surg 2018;22:508-15.
5. Papanikolaou N, Battista JJ, Boyer AL, et al. Tissue inhomogeneity corrections for megavoltage photon beams AAPM Report No 85. Madison, WI: Medical Physics Publishing, 2004.
6. Ostwald PM, Kron T, Hamilton CS. Assessment of mucosal underdosing in larynx irradiation. Int J Radiat Oncol Biol Phys 1996;36:181-7.
7. Yoon M, Lee DH, Shin D, et al. Accuracy of inhomogeneity correction algorithm in intensity-modulated radiotherapy of head-and-neck tumors. Med Dosim 2007;32:44-51.
8. Huang CY, Chu TC, Lin SY, et al. Accuracy of the convolution/superposition dose calculation algorithm at the condition of electron disequilibrium. Appl Radiat Isot 2002;57:825-30.
9. Disher B, Hajdok G, Gaede S, et al. An in-depth Monte Carlo study of lateral electron disequilibrium for small fields in ultra-low density lung: implications for modern radiation therapy. Phys Med Biol 2012;57:1543-59.
10. Disher B, Hajdok G, Gaede S, et al. Forcing lateral electron disequilibrium to spare lung tissue: a novel technique for stereotactic body radiation therapy of lung cancer. Phys Med Biol 2013;58:6641-62.
11. Martens C, Reynaert N, De Wagter C, et al. Underdosage of the upper-airway mucosa for small fields as used in intensity-modulated radiation therapy: a comparison between radiochromic film measurements, Monte Carlo simulations, and collapsed cone convolution calculations. Med Phys 2002;29:1528-35.
12. Karotki A, Mah K, Meijer G, et al. Comparison of bulk electron density and voxel-based electron density treatment planning. J Appl Clin Med Phys 2011;12:3522.
13. Hsu SH, Zawisza I, O'Grady K, et al. Towards abdominal MRI-based treatment planning using population-based Hounsfield units for bulk density assignment. Phys Med Biol 2018;63:155003.
14. Choi JH, Lee D, O'Connor L, et al. Bulk Anatomical Density Based Dose Calculation for Patient-Specific Quality Assurance of MRI-Only Prostate Radiotherapy.

Front Oncol 2019;9:997.

15. Largent A, Barateau A, Nunes JC, et al. Pseudo-CT Generation for MRI-Only Radiation Therapy Treatment Planning: Comparison Among Patch-Based, Atlas-Based, and Bulk Density Methods. Int J Radiat Oncol Biol Phys 2019;103:479-90.

16. Zhang R, Bai W, Fan X. Impact of oral contrast agent for assisting in outlining small intestine on pelvic IMAT dose in patients with cervical cancer. Medical Physics 2016;43:3364.

17. Zabel-du Bois A, Ackermann B, Hauswald H, et al. Influence of intravenous contrast agent on dose calculation in 3-D treatment planning for radiosurgery of cerebral arteriovenous malformations. Strahlenther Onkol 2009;185:318-24.

18. Maerz M, Koelbl O, Dobler B. Influence of metallic dental implants and metal artefacts on dose calculation accuracy. Strahlenther Onkol 2015;191:234-41.

19. White DR, Griffith RV, Wilson IJ. Photon, electron, proton and neutron interaction data for body tissues. International Commission on Radiation Units and Measurements, 1992.

20. Popescu CC, Olivotto IA, Beckham WA, et al. Volumetric modulated arc therapy improves dosimetry and reduces treatment time compared to conventional intensity-modulated radiotherapy for locoregional radiotherapy of left-sided breast cancer and internal mammary nodes. Int J Radiat Oncol Biol Phys 2010;76:287-95.

21. Small W Jr, Mell LK, Anderson P, et al. Consensus guidelines for delineation of clinical target volume for intensity-modulated pelvic radiotherapy in postoperative treatment of endometrial and cervical cancer. Int J Radiat Oncol Biol Phys 2008;71:428-34.

22. Gay HA, Barthold HJ, O'Meara E, et al. Pelvic normal tissue contouring guidelines for radiation therapy: a Radiation Therapy Oncology Group consensus panel atlas. Int J Radiat Oncol Biol Phys 2012;83:e353-e362.

23. Wu Q, Mohan R, Morris M, et al. Simultaneous integrated boost intensity-modulated radiotherapy for locally advanced head-and-neck squamous cell carcinomas. I: dosimetric results. Int J Radiat Oncol Biol Phys

2003;56:573-85.

24. Lomax NJ, Scheib SG. Quantifying the degree of conformity in radiosurgery treatment planning. Int J Radiat Oncol Biol Phys 2003;55:1409-19.

25. Epp ER, Lougheed MN, McKay JW. Ionization build-up in upper respiratory air passages during teletherapy with cobalt 60 radiation. Br J Radiol 1958;31:361-7.

26. Petoukhova AL, Terhaard CH, Welleweerd H. Does 4 MV perform better compared to 6 MV in the presence of air cavities in the head and neck region? Radiother Oncol 2006;79:203-7.

27. Bush K, Gagne IM, Zavgorodni S, et al. Dosimetric validation of Acuros XB with Monte Carlo methods for photon dose calculations. Med Phys 2011;38:2208-21.

28. Stathakis S, Esquivel C, Quino L V, et al. Accuracy of the small field dosimetry using the Acuros XB dose calculation algorithm within and beyond heterogeneous media for 6 MV photon beams. International Journal of Medical Physics Clinical Engineering & Radiation Oncology, 2012;1:78-87.

29. Ebert MA, Spry NA. Dose perturbation by air cavities in megavoltage photon beams: implications for cavity surface doses. Australas Radiol 2001;45:205-10.

30. Spirydovich S, Papiez L, Moskvin V, et al. Evaluation of underdosage in the external photon beam radiotherapy of glottic carcinoma: Monte Carlo study. Radiother Oncol 2006;78:159-64.

31. Dąbrowska-Szewczyk E, Zawadzka A, Kowalczyk P, et al. Influence of beam spoiler and air gap on dose distribution in build-up region for X6 MV static field. Physica Medica 2018;52:161-2.

32. Taylor M, Dunn L, Kron T, et al. Determination of peripheral underdosage at the lung-tumor interface using Monte Carlo radiation transport calculations. Med Dosim 2012;37:61-6.

33. Li XA, Yu C, Holmes T. A systematic evaluation of air cavity dose perturbation in megavoltage x-ray beams. Med Phys 2000;27:1011-7.

(English Language Editor: J. Teoh)